Modelling the active cochlea as a fully-coupled system of subwavelength Hopf resonators

H. Ammari and B. Davies

Modelling the active cochlea as a fully-coupled system of subwavelength Hopf resonators

Habib Ammari*   Bryn Davies*

Abstract

We combine recent breakthroughs in coupled resonator mechanics with the theory of cochlear Hopf resonators in order to better understand the active cochlea. We model the acoustic pressure on the surface of the basilar membrane, offering an understanding of how this couples the array of subwavelength resonators and the implications for cochlear mechanics. By decomposing the behaviour over the system's resonant modes, we are able to offer explanations for several of the inner ear's key properties, including its frequency selectivity, nonlinear amplification and two-tone response. A truncated multipole expansion is used to give efficient numerical computations.

1.1   Hopf resonators in cochlear mechanics

It is well known that the cochlea employs an active response mechanism in its function, thanks to motor proteins within its hair cells (a process known as somatic mobility) [17, 20]. Indeed, some of the cochlea's most remarkable abilities could not produced by a passive system. There is evidence that this active mechanism acts via a positive feedback loop, resulting in an amplification (or negative damping) effect [13, 23, 30]. However, the precise details of this feedback mechanism represent one of the most fundamental open questions in understanding auditory perception.

Hopf resonators have become popular objects to study thanks to their remarkable ability to account for the key properties that typify the cochlear behaviour [15, 16, 11, 17, 10, 20]. The normal form of a single Hopf resonator $z = z(t) : \mathbb{R} \to \mathbb{C}$ in the complex plane is given by the forced differential equation

---
*Department of Mathematics, ETH Zürich, Rämistrasse 101, CH-8092 Zürich, Switzerland (habib.ammari@sam.math.ethz.ch, bryn.davies@sam.math.ethz.ch).

$$\frac{\mathrm{d}z}{\mathrm{d}t} = (\mu + i\omega_0)z - |z|^2 z + F, \tag{1}$$

where $F = F(t)$ is the forcing term and ω_0 and μ are real parameters. This system is a resonator in the sense that the absolute value of the response z is greatest when the forcing F occurs with frequency ω_0.

The parameter μ is the bifurcation parameter. For $\mu < 0$ the unforced system ($F = 0$) has a stable equilibrium at $z = 0$ whereas when $\mu > 0$ this equilibrium is unstable and there exists a stable limit cycle $z(t) = \sqrt{\mu}e^{i\omega_0 t}$. This birth of a limit cycle is characteristic of a (supercritical) Hopf bifurcation. For further details see $e.g.$ [31].

The cochlea demonstrates exceptionally good frequency selectivity. Even individuals without musical training can detect tones differing in frequency by less than 0.5% [15, 8]. The excitation of system (1) at frequencies close to ω_0 is able to account for this frequency selectivity.

The cochlea is able to detect sounds with amplitudes ranging over six orders of magnitude [16, 18]. This relies on an ability to amplify sounds according to a compressive nonlinearity whereby quiet sounds are amplified much more greatly than louder ones (see $e.g.$ the experimental evidence in [26]). This property is produced by the cubic term in (1) and allows six orders of magnitude in sound amplitude to be captured by only two orders of magnitude of neural firing rates. Further, the one-third power law associated with the solution to (1) close to bifurcation (when μ is small) matches quantitatively with the responsiveness observed in the cochlea [15, 18].

A further symptom of the nonlinearity that exists in the cochlea is the behaviour that is observed under the influence of a signal composed of two distinct tones. It is firstly seen that when the ear is excited by such a stimulus two-tone suppression occurs. That is, the spectrum of the response contains the expected two amplitude peaks, however, these are smaller than each would be in the absence of the other tone [27]. Further, it has been known since the 18th century that in such a situation the ear also detects additional tones, variously known as combination tones or distortion products. First observed by the German organist Georg Sorge, these are often referred to as Tartini's tones after the Italian violinist Giuseppe Tartini [14, 25, 18]. Close to bifurcation, the nonlinearity in (1) gives products that can account for these phenomena [18, 10].

In this work we will combine the above evidence on the relevance of Hopf resonators in cochlear mechanics with recent breakthroughs in understanding the coupling between an array of hair cells [1]. We will study the acoustic pressure on the (two-dimensional) surface of the basilar membrane and will explore a model based on the standard wave equation for the propagation of sound waves, but with the addition of a "$|z|^2 z$"-inspired forcing term. A thorough discussion of the evidence supporting the modelling of hair cells as compressible elements that are excited by a pressure wave in the cochlea is given in [4], while the implications of such a model are explored in [1]. We will show that a simple model of an array of hair cells, when subjected to Hopf-type amplification and coupled by variations in acoustic pressure, can describe many of the above behaviours.
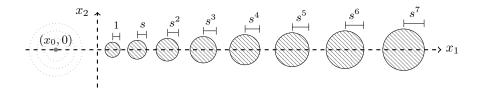
Figure 1: An array of eight (circular) subdomains $D = D_1 \cup \cdots \cup D_8$, graded in size with factor $s > 1$ and arranged linearly along $x_2 = 0$. The separation between bubbles is assumed to grow in proportion to the size. The point source is shown at $(x_0, 0) \in \mathbb{R}^2$ on the negative x_1-axis.

1.2   Problem definition

Consider a domain D in $\mathbb{R}^2$ which is the disjoint union of $N \in \mathbb{N}$ bounded and simply connected subdomains $\{D_1, \ldots, D_N\}$. Each subdomain ∂D_n such that there exists some $0 < \alpha < 1$ so that $\partial D_n \in C^{1,\alpha}$ (that is, each ∂D_n is locally the graph of a differentiable function whose derivatives are Hölder continuous with exponent α). These disjoint subdomains represent the N hair cell bundles.

We consider an acoustic pressure wave that is emitted by a point source at and is scattered by D. The point source will be located at a point $(x_0, 0) \in \mathbb{R}^2$ on the negative x_1-axis, so as to represent the signal entering the base of the cochlea. We will consider the bundles arranged in a straight line since the curvature of the cochlea does not contribute to its mechanical behaviour [9]. Figure 1 shows an example of such an arrangement, where $x = (x_1, x_2) \in \mathbb{R}^2$ represents the position on the surface of the basilar membrane.

We consider the effect of a nonlinear forcing term $\partial_t p |\partial_t p|^2$, inspired by the discussion in Section 1.1. The incoming signal is represented by a forcing term $f(t)$ at $(x_0, 0)$. We denote by ρ_b and κ_b the density and bulk modulus of the interior of the cell bundles, respectively, and denote by ρ and κ the corresponding parameters for the auditory fluid (which we assume occupies $\mathbb{R}^2 \setminus \overline{D}$). We may then denote the acoustic wave speeds in $\mathbb{R}^2 \setminus \overline{D}$ and in D respectively by

$$v = \sqrt{\frac{\kappa}{\rho}}, \quad v_b = \sqrt{\frac{\kappa_b}{\rho_b}}. \tag{2}$$

The propagation of the acoustic pressure wave $p = p(x, t)$ is then given by the problem

$$\begin{cases} \left(\Delta - \frac{1}{v^2}\frac{\partial^2}{\partial t^2}\right) p = \frac{1}{v^2} f(t)\delta_{(x_0,0)}(x), & \text{for } (x, t) \in \mathbb{R}^2 \setminus \overline{D} \times \mathbb{R}, \\ \left(\Delta - \frac{1}{v_b^2}\frac{\partial^2}{\partial t^2}\right) p = \frac{\beta}{v_b^2}|\frac{\partial p}{\partial t}|^2 \frac{\partial p}{\partial t}, & \text{for } (x, t) \in D \times \mathbb{R}, \\ p_+ - p_- = 0, & \text{for } (x, t) \in \partial D \times \mathbb{R}, \\ \frac{1}{\rho}\frac{\partial p}{\partial \nu_x}\big|_+ - \frac{1}{\rho_b}\frac{\partial p}{\partial \nu_x}\big|_- = 0, & \text{for } (x, t) \in \partial D \times \mathbb{R}, \end{cases} \tag{3}$$

where $\frac{\partial}{\partial \nu_x}$ denotes the outward normal derivative in x and the subscripts $+$ and $-$ are used to denote evaluation from outside and inside ∂D respectively. $\beta \in \mathbb{R}$ is a constant that controls the magnitude of the amplification.

3

The comparison between (3) and the standard form of a Hopf resonator (1) close to bifurcation is particularly apparent when (3) is written in the form

$$\frac{\partial^2 p}{\partial t^2} = c(x)^2 \Delta p - \beta \left| \frac{\partial p}{\partial t} \right|^2 \frac{\partial p}{\partial t} \mathcal{X}_D(x) - f(t)\delta_{(x_0,0)}(x), \quad (x,t) \in \mathbb{R}^2 \times \mathbb{R}, \quad (4)$$

where $c(x) := v - (v - v_b)\mathcal{X}_D(x)$ and $\mathcal{X}_D$ is the characteristic function of the subset $D \subset \mathbb{R}^2$. Similar formulations are considered by *e.g.* [17, 10], for the case of a single (uncoupled) Hopf resonator.

We introduce the two dimensionless contrast parameters

$$\delta = \frac{\rho_b}{\rho}, \quad \tau = \frac{v_b}{v} = \sqrt{\frac{\rho \kappa_b}{\rho_b \kappa}}. \quad (5)$$

By rescaling the dimensions of the physical problem we can assume that

$$v = O(1), \quad v_b = O(1), \quad \tau = O(1). \quad (6)$$

We also assume that the rescaled dimensions are such that the subdomains $\{D_1, \ldots, D_N\}$ have widths that are $O(1)$. On the other hand, we assume that there is a large contrast between both the bulk moduli and the density values in $\mathbb{R}^2 \setminus \overline{D}$ and in D, so that

$$\delta \ll 1. \quad (7)$$

Such an assumption is explored at length in [4], relying on experimental determinations of the Poisson ratio of hair cells.

1.3   Coupling of graded resonators

To understand the fundamental interactions between the hair cell bundles we consider the behaviour of the system of graded resonators (3) when $f = 0$ and $\beta = 0$ (*i.e.* the unforced passive problem).

We transform problem (3) into the complex frequency domain and are left with the Helmholtz problem

$$\begin{cases} \left(\Delta + \frac{\omega^2}{v^2}\right) u(x,\omega) = 0, & \text{for } (x,\omega) \in \mathbb{R}^2 \setminus \overline{D} \times \mathbb{C}, \\ \left(\Delta + \frac{\omega^2}{v_b^2}\right) u(x,\omega) = 0, & \text{for } (x,\omega) \in D \times \mathbb{C}, \\ u_+ - u_- = 0, & \text{for } (x,\omega) \in \partial D \times \mathbb{C}, \\ \delta \frac{\partial u}{\partial \nu}\big|_+ - \frac{\partial u}{\partial \nu}\big|_- = 0, & \text{for } (x,\omega) \in \partial D \times \mathbb{C}, \end{cases} \quad (8)$$

where we must also insist that $u(\cdot, \omega)$ satisfies the Sommerfeld radiation condition

$$\lim_{|x| \to \infty} |x|^{1/2} \left(\frac{\partial}{\partial|x|} - i\frac{\omega}{v} \right) u(x,\omega) = 0. \quad (9)$$

This condition is required to ensure that the solution is outgoing (rather than incoming from infinity) and gives the well-posedness of (8).

In light of the fact that (8) contains the assumption that $f = 0$, we define the *resonances* and associated *eigenmodes* of (3) to be solutions $(\omega, u(\cdot, \omega)) \in \mathbb{C} \times H^1_{loc}(\mathbb{R}^2)$ of (8). Here, $H^1_{loc}(\mathbb{R}^2)$ is the space of functions that, on every compact subset of $\mathbb{R}^2$, are square integrable and have a weak first derivative that is also square integrable (*i.e.* they are *locally* in the Sobolev space H^1). We are particularly interested in solutions where ω is small and the cell bundles are much smaller than the wavelength of the associated radiation (as is the case in with hair cells compared to the wavelength audible sound). Such solutions are known as *subwavelength* modes.

Theorem 1. *The system of N coupled resonators $D = D_1 \cup \cdots \cup D_N$ has N subwavelength resonances $\omega_1, \ldots, \omega_N$ and associated eigenmodes $u_1(x), \ldots, u_N(x)$ satisfying* (8) *with the Sommerfeld radiation condition* (9).

Proof. See [1] for details. The argument is based on representing the solution $u(x, \omega)$ to (8) as

$$u(x, \omega) = \begin{cases} \mathcal{S}_D^{\omega/v}[\psi](x), & (x, \omega) \in \mathbb{R}^2 \setminus \overline{D} \times \mathbb{C}, \\ \mathcal{S}_D^{\omega/v_b}[\phi](x), & (x, \omega) \in D \times \mathbb{C}, \end{cases} \tag{10}$$

for some surface potentials $(\phi, \psi) \in L^2(\partial D) \times L^2(\partial D)$ where $\mathcal{S}_D$ is the *Helmholtz single layer potential* associated with the domain D. This integral operator is defined as

$$\mathcal{S}_D^k[\varphi](x) := \int_{\partial D} \Gamma^k(x - y)\varphi(y)\, d\sigma(y), \quad x \in \partial D, \varphi \in L^2(\partial D), \tag{11}$$

where Γ^k is the outgoing (*i.e.* satisfying the Sommerfeld radiation condition) fundamental solution to the Helmholtz operator $\Delta + k^2$ in $\mathbb{R}^2$. $\qquad \square$

A detailed examination of the resonances and eigenmodes can be found in [1]. The crucial result is that, when the incoming signal has a wavelength that is much larger than the physical dimensions of the resonators, the behaviour of the system can be approximated by decomposing the solution over the space spanned by the subwavelength eigenmodes. In the case of audible sound (whose wavelength ranges from a few centimetres to several metres) being scattered by hair cells measuring tens of micrometres, this approximation gives a comprehensive description of the system's behaviour.

In order to improve computational efficiency, we assume in this work that the cell bundles are circular. This means that we can use the multipole expansion method, an explanation of which is provided in *e.g.* [2, Appendix C]. The method relies on the idea that functions in $L^2(\partial D)$ are, on each *circular* ∂D_i, 2π-periodic so we may approximate by the leading order terms of a Fourier series representation.

2 Coupled Hopf system

We decompose the motion of system (3) into the N subwavelength resonant modes by writing

$$p(x,t) \simeq \text{Re}\left(\sum_{n=1}^{N} \alpha_n(t) u_n(x)\right), \tag{12}$$

for some complex-valued time dependencies $\alpha_1(t), \ldots, \alpha_N(t)$.

In light of the transmission properties (across ∂D) that the eigenmodes inherit from (8), we reach the problem

$$\sum_{n=1}^{N} \left(\alpha_n''(t) + \omega_n^2 \alpha_n(t)\right) u_n(x) + f(t)\delta_{(x_0,0)}(x)$$

$$+ \beta \left(\sum_{n=1}^{N} \alpha_n'(t) u_n(x)\right)^2 \left(\sum_{n=1}^{N} \overline{\alpha_n'(t)}\, \overline{u_n(x)}\right) \mathcal{X}_D(x) = 0. \tag{13}$$

Definition 2. *Fix some large domain Q such that $D \cup \{(x_0,0)\} \subset Q$. Then define $\gamma \in \mathbb{C}^{N \times N}$ to be the square matrix with entries*

$$\gamma_{i,j} := \int_Q u_i(x)\overline{u_j(x)}\, dx = (u_i, u_j)_{2,Q}, \tag{14}$$

for $i, j = 1, \ldots, N$.

We are then in a position to take the $L^2(Q)$ product of (13) with u_m for $m = 1, \ldots, N$, reaching a system of N equations equations in t given by

$$\gamma^T \begin{pmatrix} \alpha_1'' + \omega_1^2 \alpha_1 \\ \vdots \\ \alpha_N'' + \omega_N^2 \alpha_N \end{pmatrix} + f \begin{pmatrix} (\delta_{(x_0,0)}, u_1)_{2,Q} \\ \vdots \\ (\delta_{(x_0,0)}, u_N)_{2,Q} \end{pmatrix} + \beta \begin{pmatrix} ((\sum \alpha_n' u_n)^2 \sum \overline{\alpha_n' u_n}, u_1)_{2,D} \\ \vdots \\ ((\sum \alpha_n' u_n)^2 \sum \overline{\alpha_n' u_n}, u_N)_{2,D} \end{pmatrix} = 0. \tag{15}$$

When studying (15) it will be useful to know that the matrix γ^T is invertible.

Lemma 3. *The matrix $\gamma \in \mathbb{C}^{N \times N}$ defined in (14) is invertible.*

Proof. This follows from the linear independence of the eigenmodes [1]. $\qquad \square$

2.1 Pure-tone response

Consider the case of an incoming signal that consists of a single pure tone at frequency Ω, that is, $f(t) = \text{Re}(Fe^{i\Omega t})$ for $F, \Omega \in \mathbb{R}$. In this case, we represent the solutions to (15) as $\alpha_n(t) = X_n e^{i\Omega t}$ for complex amplitudes $X_n \in \mathbb{C}$ [17, 31, 12]. This gives the coupled equations for $m = 1, \ldots, N$

$$(\omega_m^2 - \Omega^2)X_m + F \sum_{n=1}^{N} [\gamma^{-1}]_{n,m}(\delta_{(x_0,0)}, u_n)_{2,Q}$$

$$- i\Omega^3 \beta \sum_{n=1}^{N} [\gamma^{-1}]_{n,m} \left(\sum_{i,j,k=1}^{N} X_i X_j \overline{X_k}(u_i u_j \overline{u_k}, u_n)_{2,D}\right) = 0. \tag{16}$$
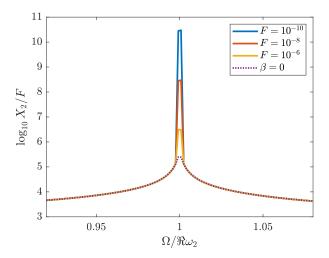
Figure 2: Nonlinear amplification in the coupled Hopf system at resonance. We show how the response X_2/F varies with incoming frequency Ω in system (16) for difference forcing magnitudes F. The response of the second eigenmode in a system of $N = 6$ cell bundles is studied. The dashed line shows the case where the cubic nonlinearity has been removed (giving a passive system) for comparison.

The results of solving (16) numerically for $X_1, \ldots, X_N$ are shown in Figure 2. There is a sharply increased response when Ω is close to the resonant frequency associated with the eigenmode. Different magnitudes of force F are shown. When the force is smaller, the response is much greater, thereby allowing the model to capture a very large range of forcing amplitudes with only relatively small variations in acoustic pressure. The sharper response of the active system will also improve frequency resolution, compared to the passive model.

In Figure 3 we study how the phase of the oscillations in the acoustic pressure lag behind the forcing, as is common in a coupled system of oscillators. This is achieved by writing the solution (12) as

$$p(x,t) \simeq \mathrm{Re}\left(\sum_{n=1}^{N} X_n e^{i\Omega t} u_n(x)\right) = \mathrm{Re}\left(R(x)e^{i(\Omega t + \phi(x))}\right), \qquad (17)$$

for real constants R and ϕ, the latter of which represents the phase delay. ϕ in (17) is, in principle, defined such that $0 \leq \phi < 2\pi$, however the assumption that ϕ should be a continuous function of Ω leads to the phase delays of multiple cycles seen in Figure 3.

The behaviour shown in Figure 3 shows many similarities to experimental observations [26, 29]. It is notable that the curves all start at a 'lag' of approximately minus a quarter cycle and the delay then increases with increasing frequency. There is a tendency for curves to group around values separated by a full cycle. Known as "phase plateaus", this behaviour has been widely observed
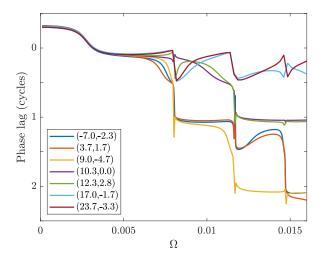
7

Figure 3: The phase-frequency relationship for the coupled Hopf system. We show how the phase lag (in cycles) varies as a function of the incoming frequency Ω at different points $x = (x_1, x_2)$ on the basilar membrane. A system of $N = 6$ cells arranged along the line $x_2 = 0$ is studied.

by experimentalists [24]. Indeed, the existence of phase lags of more than π (180°) in this model is significant since such values are not typically associated with resonant systems but are required in order to describe the cochlea (where delays of several cycles are common) [5].

2.2 Two-tone interference

Consider the case of an incoming signal composed of two pure tones. We explore this behaviour by considering forcing of the form

$$f(t) = \operatorname{Re}\left(F_1 e^{i\Omega_1 t} + F_2 e^{i\Omega_2 t}\right), \tag{18}$$

in system (15). In this case the response, captured by the complex-valued functions $\alpha_1(t), \ldots, \alpha_N(t)$, will contain contributions from all the Fourier amplitudes with frequencies $p\Omega_1 + q\Omega_2$ for integers $p, q \in \mathbb{Z}$ [18]. Thus, for each $n = 1, \ldots, N$ there exist $X_{p,q}^{(n)} \in \mathbb{C}$, $p, q \in \mathbb{Z}$ such that

$$\alpha_n(t) = \sum_{p,q=-\infty}^{\infty} X_{p,q}^{(n)} e^{i(p\Omega_1 + q\Omega_2)t}. \tag{19}$$

The expansion (19) is dominated by the terms with small $|p|+|q|$ [18, 22, 28]. As a result, it makes sense to refer to $|p|+|q|$ as the *order* of $X_{p,q}$. In particular, it is found in [28] that the amplitudes approximately obey the law $X_{p,q} \sim X_{1,0}^{|p|} X_{0,1}^{|q|}$ and thus diminish with increasing order (for small amplitudes).
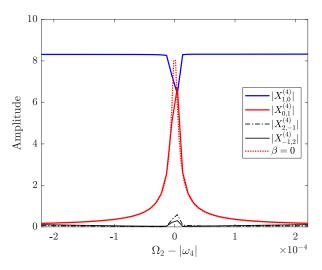
Figure 4: Two-tone interference in the coupled Hopf system. We study the fourth eigenmode in a system of $N = 6$ cells and show how the absolute values of the leading order coefficients vary in the case that $\Omega_1 = |\omega_4|$ is fixed and Ω_2 is varied. We use $F_1 = F_2 = 10^{-4}$. The red dashed line shows $X_{0,1}^{(4)}$ in the case where the cubic nonlinearity has been removed (giving a passive system) for comparison.

We substitute the expansion (19) into (15). The effect of the cubic nonlinearity is that many terms, including all those of even order, must vanish. We find that, for small amplitudes, we can approximate (19) by

$$
\begin{aligned}
\alpha_n(t) = & X_{1,0}^{(n)} e^{i\Omega_1 t} + X_{0,1}^{(n)} e^{i\Omega_2 t} \\
& + X_{2,-1}^{(n)} e^{i(2\Omega_1 - \Omega_2)t} + X_{-1,2}^{(n)} e^{i(-\Omega_1 + 2\Omega_2)t} + \dots.
\end{aligned}
\tag{20}
$$

By comparing the coefficients of the dominant Fourier modes $e^{i\Omega_1 t}$, $e^{i\Omega_2 t}$, $e^{i(2\Omega_1 - \Omega_2)t}$ and $e^{i(-\Omega_1 + 2\Omega_2)t}$ we reach a coupled system of equations that we may solve to find $\left\{ X_{1,0}^{(n)}, X_{0,1}^{(n)}, X_{2,-1}^{(n)}, X_{-1,2}^{(n)} : n = 1, \dots, N \right\}$ (for details, see Appendix A).

Figure 4 shows the amplitudes of the four dominant Fourier modes when $\Omega_1 = |\omega_4|$ is fixed and Ω_2 is varied (in the neighbourhood of $|\omega_4|$). When Ω_2 is away from $|\omega_4|$ there appears to be little interaction between the two frequency modes. As Ω_1 and Ω_2 become close, however, two phenomena emerge. Firstly, two-tone suppression occurs. This is witnessed both by the fact that the value of $X_{1,0}^{(4)}$ drops (from its otherwise constant value) and that the response of $X_{0,1}^{(4)}$ at resonance is diminished relative to the passive system (whish corresponds to $\beta = 0$ and is shown as the dashed curve in Figure 4). On top of this, so-called combination tones appear in the regime where Ω_1 and Ω_2 are close together. These are shown as the two black lines in Figure 4 and represent Tartini's famous tones.

9

3   Discussion

We have studied the acoustic pressure on the surface of the basilar membrane by combining an understanding of the coupling between an array of subwavelength resonators (described by Theorem 1) with the theory of Hopf resonators in cochlear mechanics (explored in Section 1.1). This approach has proved successful in describing several phenomena commonly exhibited by the cochlea. Firstly, it was shown in Section 2.1 that the model produced the desired frequency selectivity and nonlinear amplification. The phase lag also showed similarities to experimental observations. Then, in Section 2.2 it was further shown that the two-tone response of this coupled Hopf system both suffers from two-tone suppression and produces combination tones.

Contrary to the linear array used in this work, the arrangement of hair cells in the cochlea of a mammal takes the form of a row of inner hair cells and three rows of outer hair cells. It is believed that the outer hair cells are responsible for the forcing while inner hair cells act as receivers [7, 8]. In recent work the geometric arrangement of the hair cells has been studied in an attempt to capture the cochlea's behaviour [6, 3]. Using our numerical (layer potential) formulation, the geometry can be easily modified providing an avenue for developing such theories.

It has been known since their first observation by David Kemp in 1978 that the ear emits sounds known as otoacoustic emissions [19, 32]. This phenomenon was one of the earlier pieces of evidence supporting the active nature of the cochlea and has provided an avenue to explore its inner workings [21]. The ear even emits *spontaneous* otoacoustic emissions in the absence of external stimulation. Recent work [7, 10] has shown that a Hopf resonator can account for the production of spontaneous otoacoustic emissions by the addition of a "self-tuning" feedback loop. In our setting, this entails introducing a $\mu \partial_t p$ term to (3) and varying the parameter μ in the neighbourhood of the bifurcation. The spontaneous sounds are created when the system strays into the regime where a stable limit cycle exists.

Even with the use of the multipole method (reliant on the assumption that the cell bundles are circular) the computations in this work become expensive for large numbers of cells. In order to efficiently and concisely demonstrate the behaviour of the coupled Hopf system, the results displayed here use only small values for N. While it is feasible to study up to a few hundred cells with our current methodology, numerical computations on a model resembling a genuine mammalian cochlea (and its approximately 15,000 hair cells) are beyond the scope of our current setup. A rigorous approach to approximating the coupling between an array of subwavelength resonators would thus represent a valuable breakthrough.

A   Appendix: Two-tone interference

By writing the amplitudes $\alpha_n(t)$ in the approximate form given in (20) we are able to rewrite the decomposition of $p(x,t)$ in (12) in terms of the dominant Fourier amplitudes

$$
p(x,t) = \left(\sum_{n=1}^{N} X_{1,0}^{(n)} u_n(x) \right) e^{i\Omega_1 t} + \left(\sum_{n=1}^{N} X_{0,1}^{(n)} u_n(x) \right) e^{i\Omega_2 t}
$$
$$
+ \left(\sum_{n=1}^{N} X_{2,-1}^{(n)} u_n(x) \right) e^{i(2\Omega_1 - \Omega_2)t} + \left(\sum_{n=1}^{N} X_{-1,2}^{(n)} u_n(x) \right) e^{i(-\Omega_1 + 2\Omega_2)t},
\tag{21}
$$

from which we see that it is convenient to define the sums

$$
S_{1,0}(x) := \Omega_1 \sum_{n=1}^{N} X_{1,0}^{(n)} u_n(x), \qquad\qquad S_{0,1}(x) := \Omega_2 \sum_{n=1}^{N} X_{0,1}^{(n)} u_n(x),
$$
$$
S_{2,-1}(x) := (2\Omega_1 - \Omega_2) \sum_{n=1}^{N} X_{2,-1}^{(n)} u_n(x), \quad S_{-1,2}(x) := (-\Omega_1 + 2\Omega_2) \sum_{n=1}^{N} X_{-1,2}^{(n)} u_n(x).
$$

We then wish to compute the coefficients of the Fourier modes $e^{i\Omega_1 t}$, $e^{i\Omega_2 t}$, $e^{i(2\Omega_1 - \Omega_2)t}$ and $e^{i(-\Omega_1 + 2\Omega_2)t}$ when we substitute (21) into the nonlinearity $|\partial_t p|^2 \partial_t p$. We find that these coefficients are respectively given by

$$
C_{1,0} := S_{1,0}|S_{1,0}|^2 + 2S_{1,0}\left[|S_{0,1}|^2 + |S_{2,-1}|^2 + |S_{-1,2}|^2 \right]
$$
$$
+ S_{0,1}^2 \overline{S_{-1,2}} + 2S_{0,1}S_{2,-1}\overline{S_{1,0}} + 2S_{2,-1}S_{-1,2}\overline{S_{0,1}},
$$
$$
C_{0,1} := S_{0,1}|S_{0,1}|^2 + 2S_{0,1}\left[|S_{1,0}|^2 + |S_{2,-1}|^2 + |S_{-1,2}|^2 \right]
$$
$$
+ S_{1,0}^2 \overline{S_{2,-1}} + 2S_{1,0}S_{-1,2}\overline{S_{0,1}} + 2S_{2,-1}S_{-1,2}\overline{S_{1,0}},
$$
$$
C_{2,-1} := S_{2,-1}|S_{2,-1}|^2 + 2S_{2,-1}\left[|S_{1,0}|^2 + |S_{0,1}|^2 + |S_{-1,2}|^2 \right]
$$
$$
+ S_{1,0}^2 \overline{S_{0,1}} + 2S_{1,0}S_{0,1}\overline{S_{-1,2}},
$$
$$
C_{-1,2} := S_{-1,2}|S_{-1,2}|^2 + 2S_{-1,2}\left[|S_{1,0}|^2 + |S_{0,1}|^2 + |S_{2,-1}|^2 \right]
$$
$$
+ S_{0,1}^2 \overline{S_{1,0}} + 2S_{1,0}S_{0,1}\overline{S_{2,-1}}.
$$

It is then more straightforward to see that when we substitute (20) into system (15) and equate coefficients of the Fourier modes $e^{i\Omega_1 t}$, $e^{i\Omega_2 t}$, $e^{i(2\Omega_1 - \Omega_2)t}$ and $e^{i(-\Omega_1 + 2\Omega_2)t}$ we reach the four coupled systems given by

$$
\gamma^T \begin{pmatrix} (\omega_1^2 - \Omega_1^2)X_{1,0}^{(1)} \\ \vdots \\ (\omega_N^2 - \Omega_1^2)X_{1,0}^{(N)} \end{pmatrix} + F_1 \begin{pmatrix} (\delta_{(x_0,0)}, u_1)_{2,Q} \\ \vdots \\ (\delta_{(x_0,0)}, u_N)_{2,Q} \end{pmatrix} - i\beta \begin{pmatrix} (C_{1,0}, u_1)_{2,D} \\ \vdots \\ (C_{1,0}, u_N)_{2,D} \end{pmatrix} = 0. \tag{22}
$$

$$\gamma^T \begin{pmatrix} (\omega_1^2 - \Omega_2^2)X_{0,1}^{(1)} \\ \vdots \\ (\omega_N^2 - \Omega_2^2)X_{0,1}^{(N)} \end{pmatrix} + F_2 \begin{pmatrix} (\delta_{(x_0,0)}, u_1)_{2,Q} \\ \vdots \\ (\delta_{(x_0,0)}, u_N)_{2,Q} \end{pmatrix} - i\beta \begin{pmatrix} (C_{0,1}, u_1)_{2,D} \\ \vdots \\ (C_{0,1}, u_N)_{2,D} \end{pmatrix} = 0. \quad (23)$$

$$\gamma^T \begin{pmatrix} (\omega_1^2 - (2\Omega_1 - \Omega_2)^2)X_{2,-1}^{(1)} \\ \vdots \\ (\omega_N^2 - (2\Omega_1 - \Omega_2)^2)X_{2,-1}^{(N)} \end{pmatrix} - i\beta \begin{pmatrix} (C_{2,-1}, u_1)_{2,D} \\ \vdots \\ (C_{2,-1}, u_N)_{2,D} \end{pmatrix} = 0. \quad (24)$$

$$\gamma^T \begin{pmatrix} (\omega_1^2 - (-\Omega_1 + 2\Omega_2)^2)X_{-1,2}^{(1)} \\ \vdots \\ (\omega_N^2 - (-\Omega_1 + 2\Omega_2)^2)X_{-1,2}^{(N)} \end{pmatrix} - i\beta \begin{pmatrix} (C_{-1,2}, u_1)_{2,D} \\ \vdots \\ (C_{-1,2}, u_N)_{2,D} \end{pmatrix} = 0, \quad (25)$$

which we can solve numerically to find $\left\{ X_{1,0}^{(n)}, X_{0,1}^{(n)}, X_{2,-1}^{(n)}, X_{-1,2}^{(n)} : n = 1, \ldots, N \right\}$.

References

[1] Ammari, H. and Davies, B. (2019). A fully-coupled subwavelength resonance approach to modelling the passive cochlea. *arXiv preprint arXiv:1901.08808*.

[2] Ammari, H., Fitzpatrick, B., Lee, H., Yu, S., and Zhang, H. (2017). Subwavelength phononic bandgap opening in bubbly media. *J. Differ. Equations*, 263(9):5610–5629.

[3] Bell, A. (2002). Musical ratios in geometrical spacing of outer hair cells in the cochlea: strings of an underwater piano? In Stevens, C., Burnham, D., McPherson, G., Schubert, E., and Renwick, J., editors, *Proceedings of the 7th international conference on music perception and cognition*, Sydney. Causal Productions, Adelaide.

[4] Bell, A. (2005). *The underwater piano: a resonance theory of cochlear mechanics*. PhD thesis, The Australian National University.

[5] Bell, A. (2012). A resonance approach to cochlear mechanics. *PLoS One*, 7(11):e47918.

[6] Bell, A. and Fletcher, N. H. (2004). The cochlear amplifier as a standing wave:"squirting" waves between rows of outer hair cells? *J. Acoust. Soc. Am.*, 116(2):1016–1024.

[7] Camalet, S., Duke, T., Jülicher, F., and Prost, J. (2000). Auditory sensitivity provided by self-tuned critical oscillations of hair cells. *P. Natl. Acad. Sci. U.S.A.*, 97(7):3183–3188.

[8] Dallos, P. (1992). The active cochlea. *J. Neurosci.*, 12(12):4575–4585.

[9] Duifhuis, H. (2012). *Cochlear mechanics: introduction to a time domain analysis of the nonlinear cochlea*. Springer Science & Business Media, New York.

[10] Duke, T. and Jülicher, F. (2008). Critical oscillators as active elements in hearing. In *Active Processes and Otoacoustic Emissions in Hearing*, pages 63–92. Springer, New York.

[11] Eguíluz, V. M., Ospeck, M., Choe, Y., Hudspeth, A., and Magnasco, M. O. (2000). Essential nonlinearities in hearing. *Phys. Rev. Lett.*, 84(22):5232.

[12] Fletcher, N. H. (1992). *Acoustic systems in biology*. Oxford University Press, New York.

[13] Gold, T. (1948). Hearing. ii. the physical basis of the action of the cochlea. *P. Roy. Soc. Lond. B Bio.*, 135(881):492–498.

[14] Helmholtz, H. L. F. (1954). *On the sensations of tone*. Dover, New York.

[15] Hudspeth, A. (2008). Making an effort to listen: mechanical amplification in the ear. *Neuron*, 59(4):530–545.

[16] Hudspeth, A., Jülicher, F., and Martin, P. (2010). A critique of the critical cochlea: Hopf—a bifurcation—is better than none. *J. Neurophysiol.*, 104(3):1219–1229.

[17] Joyce, B. S. and Tarazaga, P. A. (2017). A study of active artificial hair cell models inspired by outer hair cell somatic motility. *J. Intel. Mat. Syst. Str.*, 28(6):811–823.

[18] Jülicher, F., Andor, D., and Duke, T. (2001). Physical basis of two-tone interference in hearing. *P. Natl. Acad. Sci. U.S.A.*, 98(16):9080–9085.

[19] Kemp, D. T. (2002). Otoacoustic emissions, their origin in cochlear function, and use. *Brit. Med. Bull.*, 63(1):223–241.

[20] Kern, A. and Stoop, R. (2003). Essential role of couplings between hearing nonlinearities. *Phys. Rev. Lett.*, 91(12):128101.

[21] Martin, P., Hudspeth, A., and Jülicher, F. (2001). Comparison of a hair bundle's spontaneous oscillations with its response to mechanical stimulation reveals the underlying active process. *P. Natl. Acad. Sci. U.S.A.*, 98(25):14380–14385.

[22] Montgomery, K. (2008). Multifrequency forcing of a hopf oscillator model of the inner ear. *Biophys. J.*, 95(3):1075–1079.

[23] Neely, S. T. and Kim, D. (1986). A model for active elements in cochlear biomechanics. *J. Acoust. Soc. Am.*, 79(5):1472–1480.

[24] Robles, L. and Ruggero, M. A. (2001). Mechanics of the mammalian cochlea. *Physiol. Rev.*, 81(3):1305–1352.

[25] Robles, L., Ruggero, M. A., and Rich, N. C. (1997). Two-tone distortion on the basilar membrane of the chinchilla cochlea. *J. Neurophysiol.*, 77(5):2385–2399.

[26] Ruggero, M. A., Rich, N. C., Recio, A., Narayan, S. S., and Robles, L. (1997). Basilar-membrane responses to tones at the base of the chinchilla cochlea. *J. Acoust. Soc. Am.*, 101(4):2151–2163.

[27] Ruggero, M. A., Robles, L., Rich, N. C., et al. (1992). Two-tone suppression in the basilar membrane of the cochlea: Mechanical basis of auditory-nerve rate suppression. *J. Neurophysiol.*, 68:1087–1087.

[28] Stoop, R., Steeb, W.-H., Gallas, J. C., and Kern, A. (2005). Auditory two-tone suppression from a subcritical hopf cochlea. *Physica A*, 351(1):175–183.

[29] Wilson, J. P. and Evans, E. F. (1983). Some observations on the "passive" mechanics of cat basilar membrane. In Webster, W. R. and Aitkin, L. M., editors, *Mechanisms of Hearing*, pages 30–35. Monash University Press, Clayton, Victoria, Australia.

[30] Wit, H. P. (1989). Comment on "a cochlear model for acoustic emissions"[J. Acoust. Soc. Am. 8 4, 222–229 (1988)]. *J. Acoust. Soc. Am.*, 85(5):2217–2217.

[31] Wong, C. W. (2013). *Introduction to mathematical physics: methods & concepts*. Oxford University Press, Oxford.

[32] Zurek, P. (1985). Acoustic emissions from the ear: A summary of results from humans and animals. *J. Acoust. Soc. Am.*, 78(1):340–344.